Re-Visiting Earthquake Resistant Design

Gian Michele Calvi[1], Gerard J. O'Reilly[2], Guido Andreotti[3]

[1] EUCENTRE Foundation and IUSS Pavia, Italy
[2] IUSS Pavia, Italy
[3] University of Pavia, Italy

ABSTRACT

Earthquakes have caused thousands of casualties and €billions of losses. As a reaction, the earthquake engineering community has developed approaches to predict the response of simple structures (as opposite to complete constructions) and codes of practice considering a single "life safety" performance objective, assumed to be associated with the prevention of structural collapse. Recently, the perception of different performance levels' pertinence on total losses following an earthquake has become increasingly relevant and numerous developments on the convolution of hazard-vulnerability-exposure followed to give a framework with which to quantify and manage seismic risk. However, many developments aim to correct old approaches, which are based on questionable assumptions and fail to produce consistent and effective procedures.

This keynote lecture aims to re-discuss the challenges induced by seismic demand in the constructed environment, focusing on the following main topics:

- A rational definition of earthquake-induced demand. Since many assumptions on ground motion demands are based on few records from over 50 years ago, it seems logical to revisit this and consider the plethora of digital records today available;
- A re-visitation of the connection between structural response parameters during earthquakes and resulting losses by considering damage to both structural and non-structural elements, effects of downtime, loss of competitiveness and societal impact;
- A consequent revision of seismic design philosophy and methods using the above two points' outputs. In the past, these moved from a strength–acceleration comparison, followed by a ductility-based demand–capacity check, to displacement-based approaches. A simpler and clearer approach to mitigate economic impact and protect lives during seismic events is outlined.

Keywords: design; response spectra; soil effects; performance; risk.

INTRODUCTION

One of the most fundamental aspects of earthquake engineering is the characterisation of ground shaking in a way to be of practical use when designing and assessing structures. Response spectra have played a key role in bridging this gap between dynamic structural response and static structural analysis. The traditional shape of design spectra, based on regions characterised by constant displacement, constant velocity and constant acceleration, has been questioned from a conceptual point of view by Calvi [1] and a new formulation based on magnitude and fault distance only has been proposed by Calvi *et al.* [2]. The parameters required by this formulation had been derived from some 360 ground motions recorded on rock or dense soil, originated by 24 earthquakes occurred in Italy between 1972 and 2017, with magnitude between 4.5 and 6.5. Furthermore, Calvi and Andreotti [3] have presented an extension of the approach to all types of soil, considering a much more extended set of ground motions recorded in Europe and the Middle East (6866 records, from 387 events, magnitude between 4.5 and 7.6 and stations distance between 0 and 80 km).

In addition to accounting for the impacts of soil non-linearity on the design spectrum, the impacts of different considerations regarding the correction as a consequence of structural non-linearity is an issue also recently addressed by Calvi [4]. These issues form some of the first aspects in seismic design revisited in this keynoted, followed by a description of how performance may be defined and implemented in an alternative and arguably more appropriate fashion. Since the introduction of performance-based earthquake engineering (PBEE) in 1995 [5], seismic design has undergone significant development and can be simply summarised as foreseeing building damage to different extents for increased levels of seismic shaking. This has evolved into a procedure adopted by most modern design codes, where a number of ground shaking return periods are identified and an acceptable performance associated with each one, typically termed limit states. In design codes such as Eurocode 8

(EC8) in Europe [6], ASCE 7-16 in the US [7] and NZS1170 in New Zealand [8], for example, building performance is checked through the provision of storey drift limits and member verification checks, among other requirements. This is of great convenience to engineers since it frames the seismic design problem in terms of familiar quantities like member force or storey drift and can be verified with relative ease using conventional engineering tools. However, when describing the building performance to the owner and its occupants, these quantities have relatively little significance.

From a building owner perspective, what is of immediate interest is the direct financial burden of repairing or replacing their building due to seismic damage. Also of concern are the indirect losses due to building downtime while functionality is being restored. From a building occupant point of view, the safety of the building and the risk of casualty are of more immediate concern. These aspects form part of what has been become known as the Pacific Earthquake Engineering Center (PEER) PBEE methodology initially outlined by Cornell and Krawinkler [9]. This represented an evolution to the initial meaning of the term PBEE whereby performance quantities were framed in a more probabilistic manner. It paved the way for a new definition of building performance using metrics that were of more direct meaning to building owners and occupants, and led to guidelines like FEMA P58 [10] being developed. It allows the performance of existing buildings to be quantified in terms of metrics like expected annual loss (EAL) and mean annual frequency of collapse (MAFC), as illustrated in Figure 1. However, this framework and its associated guidelines have mainly been focused on assessment of existing buildings rather than the sizing and design of new ones.

In practice, the seismic design process can be divided into three general phases: 1) the identification of a suitable lateral load resisting system and its associated geometrical layout; 2) the detailing of structural members for forces and deformations identified using one of many available seismic design methods; and 3) the performance verification of the resulting design using either linear or non-linear, static or dynamic analysis. For the second phase, many seismic design methods exist to adequately identify the structural demands for a given definition of seismic input. Similarly for the third phase, where current design codes typically prescribe different performance acceptance criteria defined in terms of strength, stability and limit state verifications, among others. However, before either of these two phases can be concluded, the lateral load resisting system and its associated geometrical layout are required. This aspect is not given much attention in current seismic design codes and is generally left to designer experience in consultation with the client's and architect's requirements. Given the key role structural typology plays, it seems logical that some kind of guidance be given to designers who know what kind of performance they and the client require, but are left to an almost trial and error approach - usually refined with experience - when it comes to selecting a structural system.

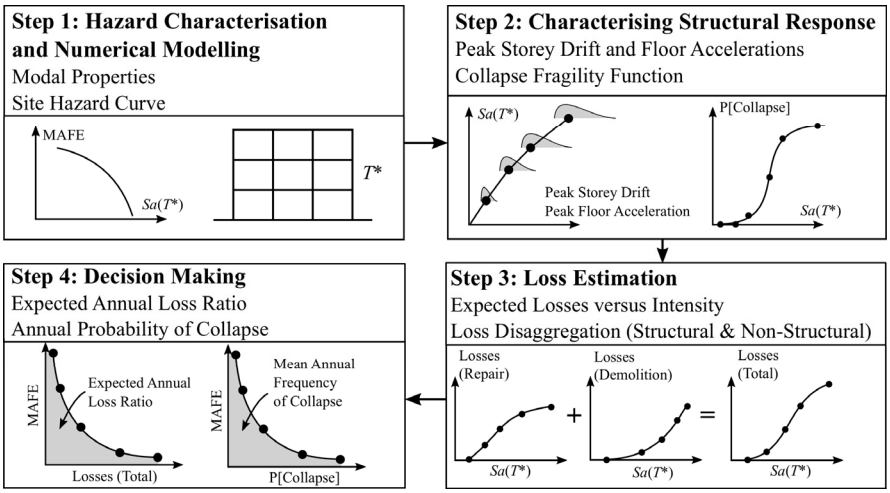

Figure 1. Overview of the PEER PBEE framework used to estimate the EAL and MAFC of an existing building (adapted from O'Reilly et al. [11]*). Note: MAFE denotes mean annual frequency of exceedance, whereas Sa(T*) refers to the spectral acceleration at a period T*.*

What is largely absent in PBEE up to now is a comprehensive design framework that can aid designers during the first phase of seismic design, where the structure is conceived conceptually or different strengthening measures decided on in the case of retrofitting. Thus, a framework that focuses on the first phase of design, keeping the performance objectives of the third phase closely in mind, whilst utilising the well-developed methods of structural detailing in phase two is largely absent. This paper outlines a novel framework that addresses this first phase, as discussed by O'Reilly and Calvi [12], which has largely been left undeveloped, whereby structural systems can be identified utilising more meaningful performance metrics like EAL.

DEFINING THE SEISMIC ACTION

Shape of design spectra

A critical revisitation of design spectra has been conceptually presented by Calvi [1] and rational design spectra shapes have been derived by Calvi *et al.* [2] as a function of magnitude and fault distance, based on about 360 ground motion signals recorded in Italy over the past fifty years. The concepts and procedures described in these papers have been further refined and extended to consider the effects of different local soil conditions by Calvi and Andreotti [3], analysing 6866 records generated by 387 different events. The basic issues of the design spectra obtained are summarised in Figure 2. Essentially, the spectral regions characterised by very low and very high periods of vibration are neglected, as irrelevant for design and each spectrum is defined by two regions at peak spectral acceleration and displacement demands and by an intermediate region where both acceleration and displacement vary non-linearly. This intermediate region corresponds to what was defined as the "constant velocity" part of the spectrum – a concept with no physical basis [1] and has thus been abandoned in this approach.

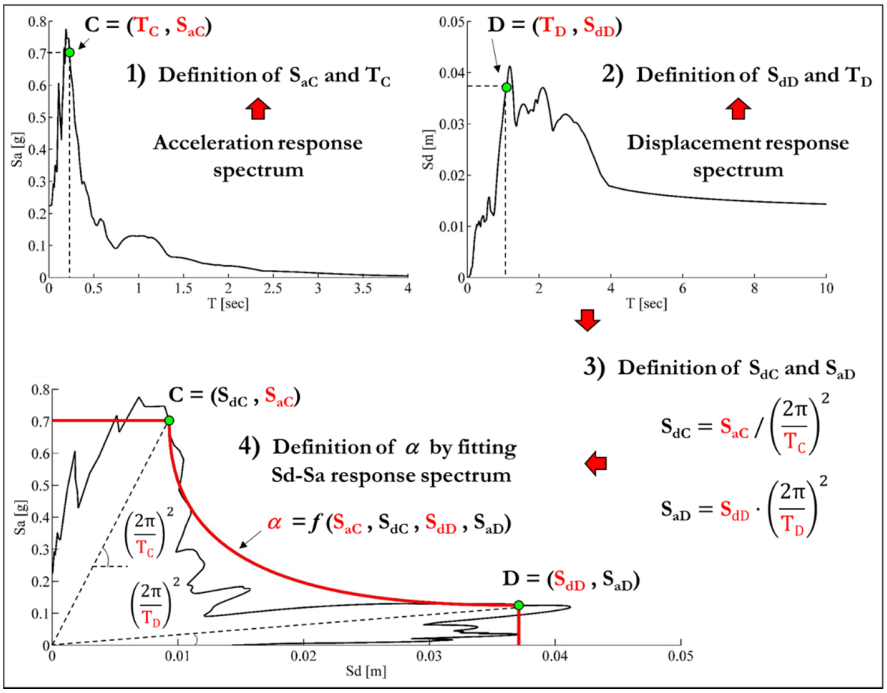

Figure 2. Procedure for the definition of the five empirical data (text highlighted in red) required to define the design spectrum proposed by Calvi [1] *and Calvi et al.* [2]*; from Calvi and Andreotti* [3].

Effects of local soil on design spectra

The analysis of the response spectra obtained for different soil types at different distances from the fault for different magnitude earthquakes in Calvi and Andreotti [3] has clearly indicated that softer soils have the general tendency to amplify the displacement demand. For what concerns the acceleration demand, there is a tendency to amplify for large distance records and to reduce for short distances from the fault, as shown Figure 3. This effect is not new, though possibly forgotten in many numerical studies. It is connected to possible non-linear response of the local soil, more likely for softer soils at shorter distances and for larger magnitude events [13–15].

A meaningful example of such tendencies is depicted in Figure 3, where the correcting factor to be applied to spectra referring to rock soils is expressed with reference to near and far field records for different soils and considering both acceleration and displacement. The general trend of the data suggests that close to the source, the amplification of peak spectral accelerations tends to decrease with magnitude for all soil classes, with higher acceleration values in case of stiffer soils. At large distances from the source, the trend is reversed with amplification factors increasing with magnitude and in case of softer soils. Displacement amplification factors in close proximity increase with magnitude and in case of softer soil, showing an opposite tendency with respect to acceleration.

The patterns found in the empirical data fit well a physical interpretation of the problem based on non-linear soil amplification despite the fact that several other phenomena may be involved (e.g. resonance phenomena, basin effects, wave scattering, inelastic attenuation, directivity effects, etc.). Near the seismic source, the non-linear response of soil is actually more

pronounced and the level of amplification is thus influenced by the degradation of the mechanical properties. The higher the shear strain demand, the greater the decrease of the shear modulus of the soil, with a consequent limitation of acceleration with magnitude and an increasing displacement. Soft soils are generally characterised by larger deformations and the response tends to be more non-linear than in stiff soils and rock, consequently, in proximity of the seismic source, the spectral acceleration decrease with magnitude and increase with stiffness whereas, for spectral displacements, there is the opposite tendency.

The amplification factors recommended by EC8 [6] are reported as a comparison, showing that these effects are neglected in this code, with both the magnitude and general trends not being at all representative of what has been found from the study by Calvi and Andreotti [3].

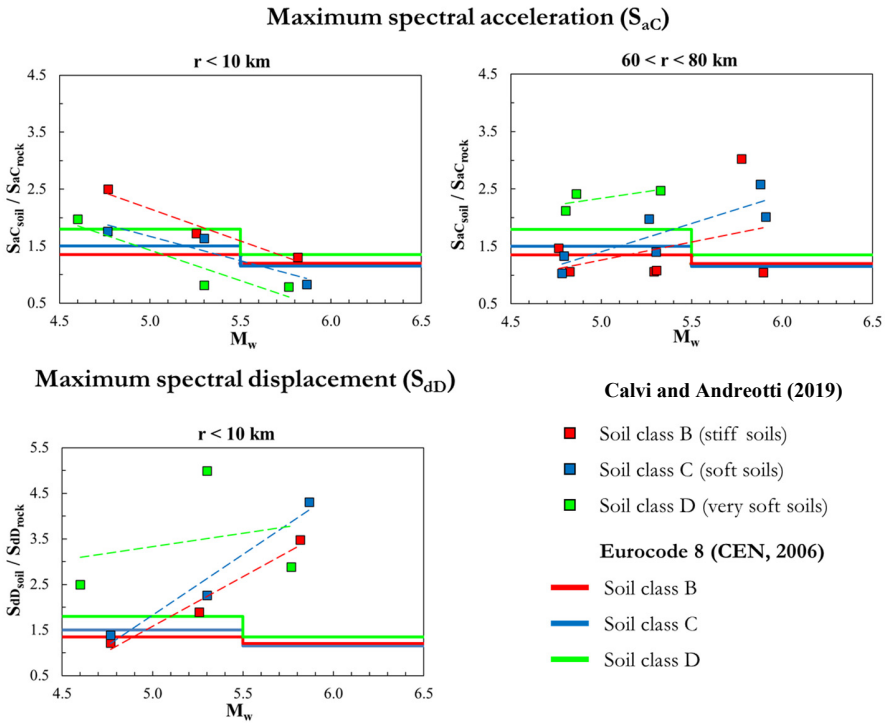

Figure 3. Variation of soil amplification factors with magnitude, distance and type of soil and comparison with S factor of Eurocode 8 (from Calvi and Andreotti [3]*).*

Design spectra

An example of response spectra obtained applying the expressions defined in Calvi and Andreotti [3] are reported in red in Figure 4, for distance shorter than 10 km or between 20 and 30 km, for magnitude between 6.0 and 6.5 or between 5.0 and 5.5 and for three cases of soil. A comparison with response spectra computed from the recorded ground motions and the response spectra derived from the ground motion prediction equation (GMPE) of spectral acceleration for Europe and the Middle East by Akkar *et al.* [16] is also illustrated. Response spectra at different percentiles are reported: the mean of the ground motions, at plus-one-standard-deviation ($+1\sigma$) and at plus-two-standard-deviation $+2\sigma$. The standard deviation is magnitude-dependent and it is computed multiplying the expected value by the appropriate coefficient of variation (CoV).

It is immediate to observe that the spectral shape in the intermediate region seem to differ significantly from a constant velocity shape meaning that the demand prediction may be very different. A comparison with code design spectra is not straightforward, but relevant differences are also expected. A second general observation, not derived from the figures shown, but rather by the analysis of empirical and predictive data, seem to indicate that distance and magnitude may affect displacement demand much more than acceleration demand, confirming that it may be improper to derive the first from the second simply counting on a regular variation, such as that imposed by a constant velocity assumption. It is evident that an event with magnitude between 5.0 and 5.5 at 30 km from the epicenter could still induce response acceleration of the order of 0.40g, while the displacement demand would be in all cases limited to a few millimeters.

While the level of protection to be provided to new or existing structures is a matter of choices to be based on probabilistic seismic hazard assessment, the observation above could be relevant in themselves for design and assessment.

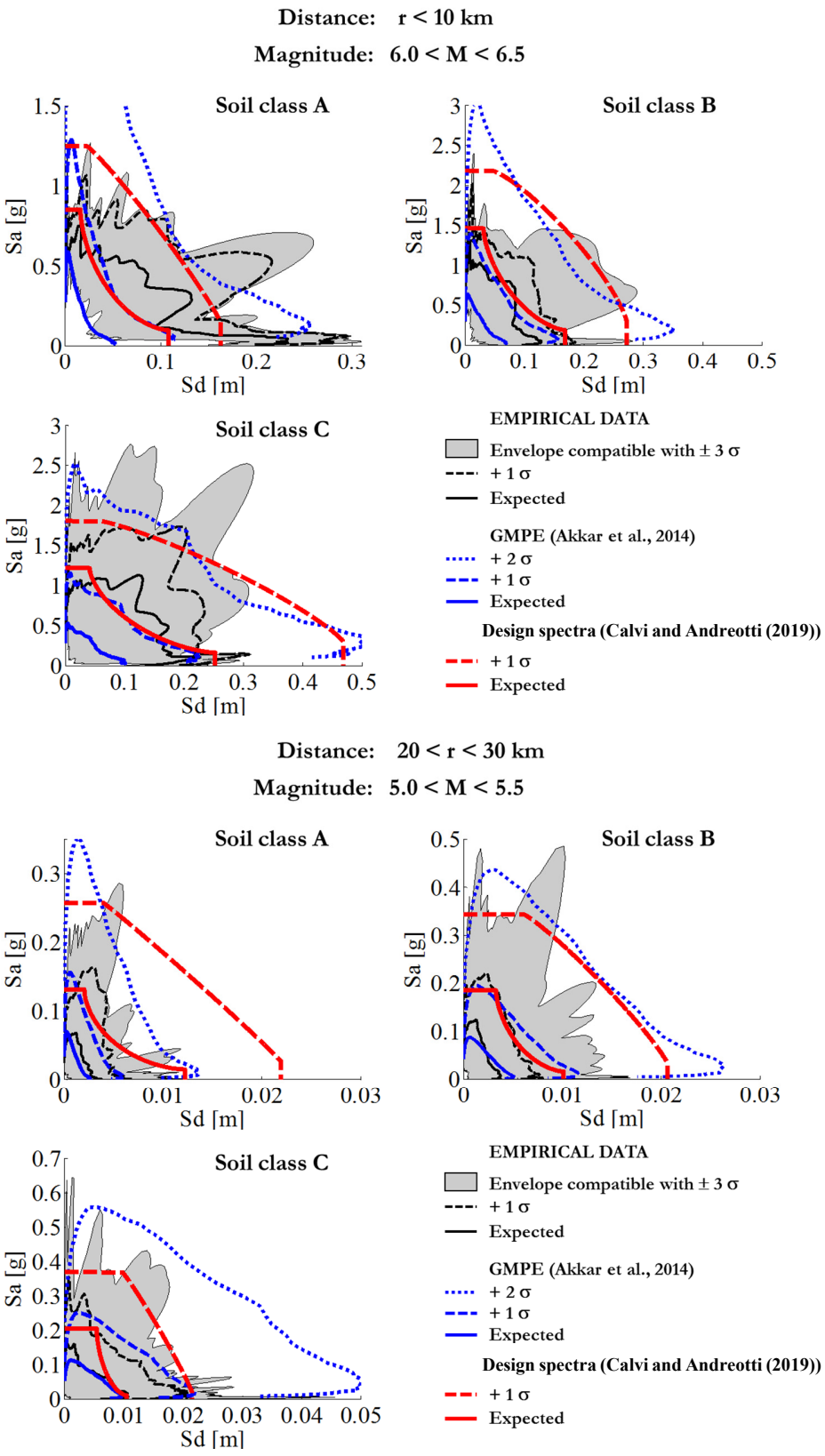

Figure 4. Comparison between design spectra proposed by Calvi and Andreotti [3]*, derived from the GMPE by Akkar et al.* [16] *and response spectra empirically derived from signal analysis.*

Accounting for energy dissipation

In the 1970s, the basic idea to derive inelastic spectra from their elastic counterpart was based on defining period ranges of the spectrum where acceleration, velocity and displacement were assumed to be "conserved" or modified by some correction factor [17]. The crucial factor with which to base the spectral correction was identified as the displacement ductility value, μ. For example, Newmark and Hall [18] recommended to derive inelastic acceleration spectra from their elastic counterparts dividing the value of the elastic acceleration by μ at low frequencies and by $(2\mu-1)^{0.5}$ at intermediate frequencies (2-8 Hz), while maintaining the elastic acceleration at high frequencies. The inelastic displacements were then obtained multiplying all the inelastic acceleration values by μ.

This approach has been discussed and modified in minor aspects, but essentially used in its basic structure in all force-based approaches (and as such in all codes of practice) to date. The most relevant conceptual modification has been to introduce a *force reduction factor* (or *behaviour factor*) still based primarily on the ductility demand, but influenced also by the structure dissipation capacity, though not necessarily in a rigorous way. In general, force reduction factors defined in different codes of practice are applied to reduce the acceleration demand, while the displacement demand is typically considered identical in linear and non-linear response, applying the so-called *equal displacement* approximation, with the exception of very short period structures.

Different approaches to design, such as the *direct displacement-based seismic design* [19], or assessment, such as those derived from the *capacity spectrum method* [20], propose to describe the structure in terms of an equivalent single degree of freedom (SDOF) model representing the fundamental inelastic mode of response in the direction considered. In these cases, the non-linear response is included in the model and only different energy dissipation capacities should be considered to reduce the displacement demand with respect to the elastic case. Typically, the energy dissipation capacity is expressed in terms of some equivalent damping, ξ_e, and a displacement reduction, η_ξ, is calculated as a function of ξ_e (as qualitatively shown in Figure 5) and applied to the elastic response spectrum.

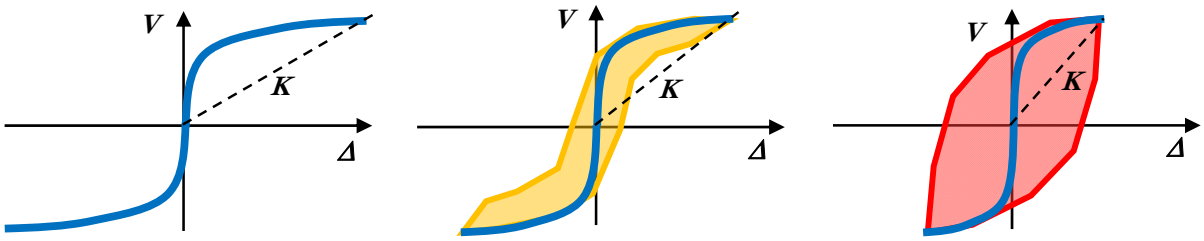

(a) Non-linear elastic response (ξ_e=5%, η_ξ = 1)

(b) Moderately dissipative structure (ξ_e=15%, η_ξ =0.75)

(c) Highly dissipative structure (ξ_e=26%, η_ξ = 0.5)

Figure 5. Effect of an increasing dissipation capacity on the expected displacement demand for the same sets of ground motions.

However, considering for simplicity the response of an existing structure, as shown in Figure 6(a) and discussed in Calvi [4], it is straightforward to realise that the reduced displacement demand induced by an increasing damping is conceptually associated with a constant shear force demand and a correspondingly increasing secant stiffness and associated period of vibration. As such, with reference to Figure 6(a), the effect of dissipation is to bring back point A (the demand in case of elastic non-dissipative response) to point B (same force, higher stiffness; green arrow), rather than to point C (same stiffness, lower force; yellow arrow).

Correcting the elastic spectrum applying the same displacement reduction factor, but keeping either the period of vibration or the spectral acceleration constant leads to quite different inelastic spectra, as shown in Figure 6(b). The black solid line defines the assumed elastic spectrum, while the red and green solid line spectra are obtained applying displacement reduction factors η_ξ = 0.75 (ξ_e=15%) and η_ξ = 0.5 (ξ_e=26%) conserving the period of vibration (i.e. both acceleration and displacement are reduced). The corresponding dotted lines are obtained for the same cases, but conserving the acceleration (i.e. only the displacement is reduced). It is evident that a pushover capacity curve, shown in orange in Figure 6(b), will cross the demand spectra at quite different displacement values, thus resulting in different required capacities.

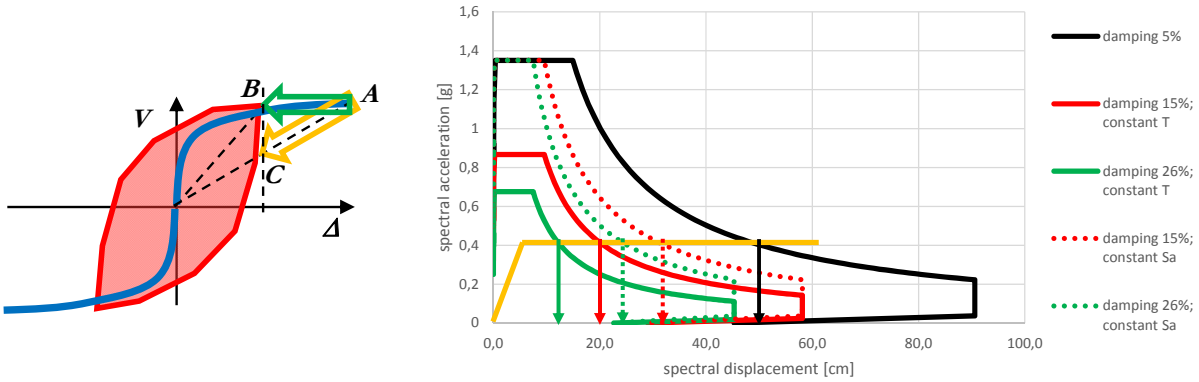

(a) *(b)*

Figure 6. Capacity spectrum assessment of a structure with assumed shear strength equal to 40 % of its effective weight, for different equivalent damping and correction of the displacement spectrum

DEFINING ACCEPTABLE PERFORMANCE

Revisiting the items discussed in the previous section regarding the characterisation of a design spectrum and account for the effects of both local soil conditions and structural non-linearity on this spectrum, it is clear that some alternative points of view that are arguably more logical to those adopted to date exist and can be further developed into a more rational approach to seismic design and assessment. In this section, attention is turned from the characterisation of seismic demand on structures to how acceptable levels of performance may be defined in order to arrive at more rational ways of designing new constructions.

Design for life safety, check for damage limitation

Current codes tend to define the seismic design problem primarily in terms of ensuring the life safety of its occupants. That is, mitigating collapse becomes the primary objective, whereas performance at frequent levels of shaking is subsequently checked. These are termed the '*no-collapse requirement*' (NC) and '*damage limitation requirement*' (DL) in the current version of EC8 [6] and correspond to ground shaking return periods, T_R, of 475 and 95 years, respectively, for a normal building importance class. Following the steps of the lateral force method shown in Figure 7, for example, a lateral load-resisting system is chosen by the designer, its behaviour factor, q, identified and the design forces determined based on some empirical estimate of initial period, T_1. These design forces are subsequently used to size and detail the structural members of the chosen lateral load-resisting system.

This approach has become known as force-based design (FBD), due to forces being the quantity that drive the procedure and its limitations have been well-documented in the literature [21]. It results in a design process whereby the design quantity of interest (i.e. displacement demand, D) is checked to be less than some prescribed capacity, C, meaning D/C simply needs to less than one. Thus, there is no real differentiation between solutions that grossly overdesign (i.e. D/C=0.2) and solutions that fall just inside the acceptance criteria (i.e. D/C=0.99). This is not to suggest that the average engineer does not strive to achieve design efficiency but rather to highlight that the code acceptance criteria do not require them to and overdesigns may result in the name of conservatism and safety. The consequence of this is that the performance of two structures designed by different engineers with differing attitudes to design efficiency, characterised via the PEER PBEE framework shown in Figure 1, will greatly differ despite them both satisfying the same initial design criteria.

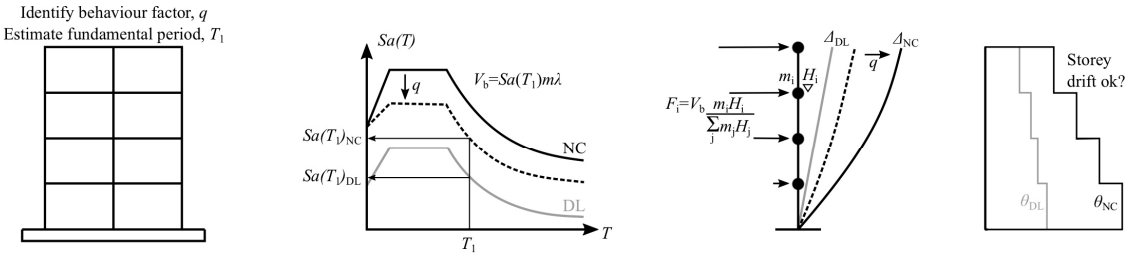

(a) Choose lateral load-resisting system (b) Identify design actions (c) Distribute forces and analyse (d) Check design

Figure 7. Basic steps of FBD as prescribed by the current version of EC8, where (a) the lateral load-resisting system is chosen, (b) design actions are identified for two limit states, DL and NC, (c) the structure is sized using the design lateral forces, F, and (d) the suitability of drift demands, θ, are checked.

Displacement-based design (DBD) was proposed as an alternative to FBD, whereby the displacement demand is set as the prescribed limit or capacity (i.e. *D=C*) at a certain level of seismic shaking, illustrated in Figure 8. This gave a simple and direct method of seismic design which culminated in the development of direct displacement-based design (DDBD) described in Priestley *et al.* [19]. This was proposed as a suitable alternative to FBD as it possesses advantages in terms of design approach and it is arguably better aligned for the objectives of PBEE, whereby performance levels can be linked to levels of structural demand rather than forces.

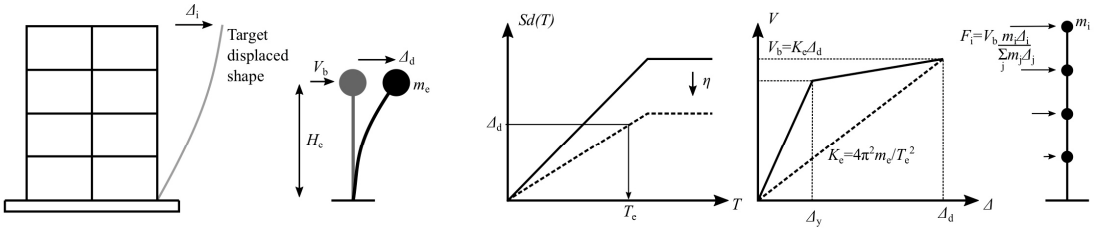

(a) Choose lateral load-resisting system and set displaced shape (b) Convert to equivalent SDOF (c) Effective period of equivalent SDOF (d) Equivalent SDOF properties (e) Design forces of MDOF

Figure 8. Basic steps of DDBD [19]*: (a) lateral load-resisting system is chosen and target lateral displacement profile set (b) equivalent SDOF system identified, (c) effective period, T_e, is identified, (d) design base shear, V_b, is identified and (e) lateral forces, F, distributed.*

Regardless of which approach is used, some aspects of building performance at other levels of seismic shaking tend to be left wanting. This arises from how design methods are set up to provide life safety at a single intensity of shaking and subsequently check the other limits as secondary aspects. For example, EC8 describes how the '*no-collapse requirement*' can be considered satisfied if the design action is less than the design resistance along with some other requirements regarding ductility, stability and capacity design. The '*damage limitation requirement*' is then considered satisfied if storey drift limits are met, whose values range between 0.5-1.0% depending on non-structural element typology and building importance class. Some non-structural element damage is related to drift demand but these only make up a portion of the economic losses. For example, Taghavi and Miranda [22] have shown that a significant portion of loss is associated with acceleration-sensitive components. In this regard, modern design codes offer no direct protection at the design stage for such elements. Furthermore, the storey drift limits currently in place in EC8, for example, have been shown by Welch and Sullivan [23] to be rather ineffective at mitigating damage to interior gypsum partitions when assessed using a PEER PBEE-oriented approach.

Lastly, it is noted that one of the first steps prior to using either FBD or DDBD is to identify a lateral load-resisting system and building geometry. It has already been noted that while this is a primary step in the seismic design process, design codes do not provide any indication on suitable choices of lateral load-resisting system at the outset of the design process.

Using EAL as a design tool

The points raised above indicate the need for a design approach that considers both peak storey drift (PSD) and peak floor acceleration (PFA) sensitive non-structural elements and the lateral load-resisting system. The simplest solution would be to adapt current design methods to account for these. But how? FBD is a simplified design process whereby a lateral force is identified and designed for, where PSD and PFA demands are then evaluated, with subsequent iterations if required. As Priestley *et al.* [19] noted, DDBD is a direct method focusing on PSD demands to make it more suited to PBEE. Therefore, should it be possible to extend DDBD to account for PSD and PFA demands in a more direct manner, this would be a significant improvement.

The focus herein is on how performance objectives are actually established. That is, how can the performance of a building defined using more advanced measures be translated into design quantities? EAL has been predominantly used in assessment and forms part of the seismic classification framework recently introduced in Italy [24]. This framework initially postulated by Calvi *et al.* [25] proposed EAL as a metric that can be used to classify a building's seismic performance. It is analogous to the energy consumption scale used in Europe that provides a simple and objective way to quantify the relative performance of different electrical appliances. Again, this framework was primarily targeted towards the assessment of existing buildings and provides a metric with which improved performance can easily be demonstrated, but its general implications were clear: EAL may be used in the seismic design and assessment process.

CONCEPTUAL SEISMIC DESIGN

With these thoughts in mind regarding the use of EAL as a tool with which to guide the design of new structures, this section will focus on an overview of a recently developed conceptual seismic design framework outlined in O'Reilly and Calvi [12]. In brief, it guides the designer towards feasible structural solutions depending on the performance objectives defined at the outset.

Identification of building performance requirements

To identify structural performance limits using EAL, consider the expected loss ratio (ELR), y, versus MAFE, λ, shown in Figure 9. ELR is the expected value of direct monetary losses arising from building damage normalised by its replacement cost. MAFE is the mean annual frequency of a limit state being exceeded and should not to be confused with the mean annual frequency of exceeding a certain level of ground shaking (i.e. a site hazard curve). To maintain a level of generality with respect to different design codes, three limit states are utilised herein:

- OLS: fully operational limit state;
- SLS: serviceability limit state;
- ULS: ultimate limit state.

SLS and ULS are aimed at ensuring satisfactory performance at lower and higher levels of ground shaking, respectively. The OLS performance point describes the point when direct monetary losses begin to accumulate due to building damage. These are shown in Figure 9 with respect to their anticipated ELR and MAFE. Based on qualitative performance expectations, ELRs may be tentatively defined as y_{OLS}=1%, y_{SLS}=15% and y_{ULS}=100%, for example. Referring to the seismic classification guidelines recently introduced in Italy [24], which were compiled based on building loss data collected following the 2009 L'Aquila earthquake [26], these ratios are deemed representative given their qualitative descriptions. Defining a non-zero value of y_{OLS} recognises that while losses may be induced for very small events, there will typically be a lower bound threshold below which insurers will not pay out premiums. While a value of 1% is set here, further studies may look to refine this value using both numerical analysis and data from past events. Adopting a value of y_{ULS}=100% implies that the building is completely unrepairable and must be replaced but is distinct from the complete collapse of the building resulting in the loss of life. Lastly, the value of y_{SLS} tentatively proposed here is aimed at defining the point at which the building starts to accumulate significant loss (i.e. >10%). More recent parametric studies by Shahnazaryan *et al.* [27] has investigated the impact of these limit state choices on the design EAL and resulting structural design. The ELR values discussed above refer exclusively to direct monetary losses and indirect losses are discussed further in Figure 17.

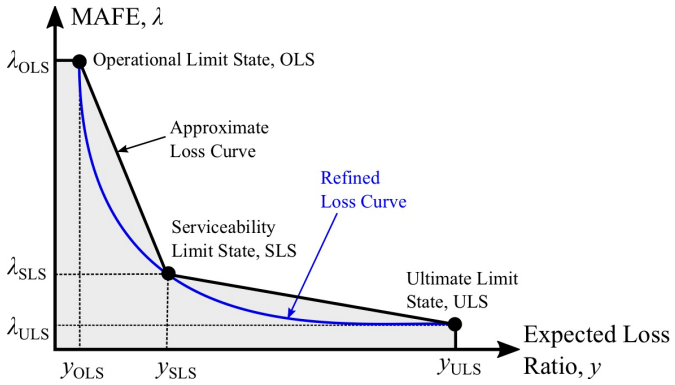

Figure 9. Illustration of approximate and refined loss curves, where integrating the expected loss ratio, y, with MAFE, λ, gives the design EAL. Note: the vertical axis is plotted using a logarithmic scale for illustration purposes.

Figure 9 is noted to possess just three performance points. This simplification is made in recognition that while more performance points on the approximate loss curve shown in Figure 9 may be desirable, a balance between simplicity and

accuracy is sought. The EAL may be approximated as the area beneath the approximate loss curve shaded in grey. This is termed approximate as more points may be added to give a more refined curve, like that shown in blue. This aspect requires careful consideration because the difference in area between the approximate and refined loss curve may appear insignificant due to its log scale. However, it can be easily shown that this area between the two curves can result in an EAL overestimation of up to 50%. This overestimation may be overcome using a closed-form expression such as the following:

$$\lambda = c_0 \exp[-c_1 \ln y - c_2 \ln^2 y] \tag{1}$$

where the coefficients c_0, c_1 and c_2 can be simply fitted to pass through the three limit state points shown in Figure 9.

Previous sections have outlined more rational ways in which design spectra may be identified for a given site and soil conditions. With this in mind, it is then necessary to identify which intensity of ground shaking each limit state needs to be designed for to satisfy the defined performance objectives and integrated within the PEER PBEE-oriented framework. A closed-form solution for the MAFE of a limit state, λ, is described by Cornell *et al.* [28] as:

$$\lambda = H(\hat{s}) \exp[0.5 k_1^2 \beta^2] \tag{2}$$

where $\hat{s}$ is the median value of the intensity measure, s, for a given limit state exceedance, k_1 is a site hazard term for the hazard curve, H, and β is the dispersion related to the limit state intensity. For example, Pinto and Franchin [29] pointed out that λ can be expected to be ~2.25 times greater than $H(\hat{s})$ for some typical values of the β and k_1. This is illustrated in Figure 10, whereby the overall impact is that there is a general shift upward of the MAFE due to the amplification of λ with respect to the $H(\hat{s})$.

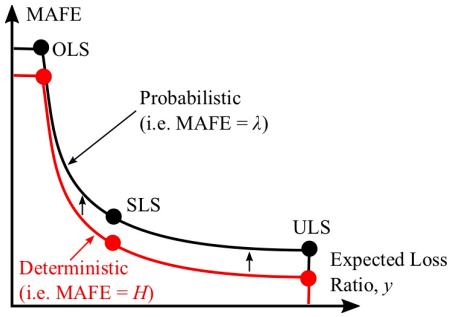

Figure 10. Impact of considering the limit state exceedance in a deterministic or probabilistic fashion.

The approach utilised herein is to adopt a set of return periods for each limit state and approximate the MAFE using Equation (2). Starting with an initial set of limit state return periods, the design EAL from Equation (1). If this value is deemed to be unsatisfactory, they should be modified accordingly and the required return period of ground shaking, T_R, can be back-calculated by inverting Equation (2). Knowing these return periods of ground shaking, the elastic design spectra could then be identified using the methods outlined in previous sections.

The SLS and ULS points are used to identify suitable maximum PSD, θ_{max}, and PFA, a_{max}, limits for design. To do this, information relating the accumulation of direct monetary losses with respect to increasing structural demand are required. Ramirez and Miranda [30] developed storey loss functions, where the damageable elements are divided into distinct groups, illustrated in Figure 11: PSD-sensitive structural elements, $y_{S,PSD}$; PSD-sensitive non-structural elements, $y_{NS,PSD}$; and PFA-sensitive non-structural elements, $y_{NS,PFA}$. These are expressed as a ratio to the saturating direct loss of each damageable group of a single storey in Figure 11, Y, which total unity (i.e. $Y_{S,PSD}+Y_{NS,PSD}+Y_{NS,PFA}=1.0$) and corresponds to the proportion, or weighting value, of each element group.

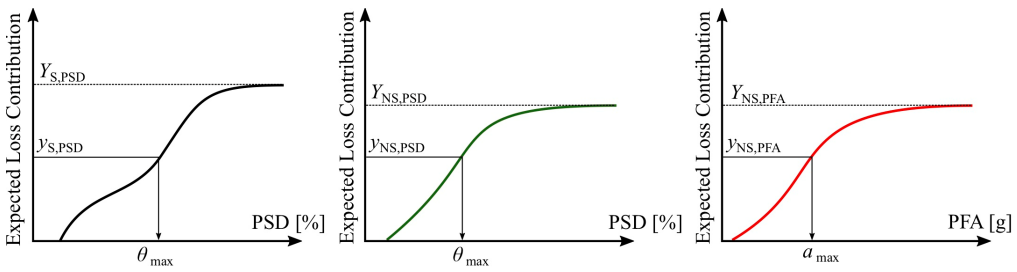

(a) PSD-sensitive structural elements

(b) PSD-sensitive non-structural elements

(c) PFA-sensitive non-structural elements

Figure 11. Identification of limit state design parameters using storey loss functions.

To link the ELR at each limit state illustrated in Figure 9 to a structural demand parameter via the storey loss functions illustrated in Figure 11, some assumption needs to be made regarding the relative weights, *Y*. For example, take a single storey structure designed not to exceed the specified ELR at a certain limit state. This means that the ELR at that performance limit state is described by:

$$y_{S,PSD} + y_{NS,PSD} + y_{NS,PFA} = y \tag{3}$$

which is the sum of all sources of loss. From Equation (3), the following can be written:

$$y_{S,PSD} = yY_{S,PSD}, \qquad y_{NS,PSD} = yY_{NS,PSD}, \qquad y_{NS,PFA} = yY_{NS,PFA} \tag{4}$$

meaning that the individual values of damageable element group loss (i.e. $y_{S,PSD}$, $y_{NS,PSD}$ and $y_{NS,PFA}$) to be entered into the respective subplots of Figure 11 can be computed as a product of the target ELR, y, and the relative weighting, Y. By entering the vertical axes Figure 11(a), (b) and (c), these will return two values of θ_{max} and a single value of a_{max} not to be exceeded in order to maintain that level of expected loss. Taking the smaller of the two θ_{max} values, which will in most cases be that associated with $y_{NS,PSD}$, the design demand parameters are therefore established.

Identification of feasible structural solution

Having defined acceptable building performance, the task remains to arrive at a feasible structural solution. Note that this implies more than one design solution (i.e. lateral strength, stiffness and ductility) and structural system (i.e. RC frame, RC wall, steel braced frame) may be possible for the design constraints identified. Potential solutions can be identified this way without committing to a specific lateral loading system. This aspect is particularly useful in aiding the conceptual seismic design stage of the construction process, where engineers present architects and clients with a range of suitable structural systems they are confident will work within the given seismic performance constraints but have not yet conducted any detailed analysis.

The first stage of any design process is to have some basic building information. Very little information is required since it is still at the conceptual design stage but information regarding the number of storeys, storey heights and seismic weight of each floor is required. Since the structure is still being conceptually designed, the total weight of each floor is not yet known. The live load is given by the design code, but the dead load is mainly a function of the slab system, which has not yet been decided. A trial dead load value may be adopted to be combined with the live load, but it is noted that this too may become a design variable to be optimised at this conceptual stage of design. For instance, designers may preliminarily investigate the usage of more advanced lightweight slab systems to reduce the dead load instead of heavier traditional slabs systems when excessive mass becomes a problem.

The next step is to convert the maximum PFA, a_{max}, and maximum PSD, θ_{max}, to spectral accelerations and displacements, which are denoted a_{SLS} and $\Delta_{d,SLS}$ for the SLS, respectively. Starting with PSD, an equivalent SDOF system is employed to characterise a first-mode dominated multi-degree of freedom (MDOF) system. This is similar to the approach adopted in DDBD where the displacement of the equivalent SDOF system is given by:

$$\Delta_d = \frac{\sum_{i=1}^{n} m_i \Delta_i^2}{\sum_{i=1}^{n} m_i \Delta_i} \tag{5}$$

where n is the number of floors in the building, with mass m_i at each floor level i and the displaced shape is denoted as Δ_i. While the floor mass is known, the displaced shape is structural system-dependant. For typical structural systems illustrated in Figure 12, these displaced shapes are described in Priestley *et al.* [19] as follows:

RC Frames
$$\Delta_i = \omega_\theta \theta_{max} H_i \left(\frac{4H_n - H_i}{4H_n - H_1}\right) \tag{6}$$

RC Walls
$$\Delta_i = \omega_\theta \begin{cases} \dfrac{\theta_{max} H_i^2}{H_n}\left(1 - \dfrac{H_i}{3H_n}\right), & \mu < 1 \\ \dfrac{\epsilon_y H_i^2}{l_w}\left(1 - \dfrac{H_i}{3H_n}\right) + \theta_p H_i, & \mu \geq 1 \end{cases} \tag{7}$$

Braced Frame
$$\Delta_i = \omega_\theta \theta_{max} H_i \tag{8}$$

where μ is the level of ductility, H_i is the i^{th} floor's elevation above the base, ε_y is the yield strain of the reinforcement, l_w is the RC wall length, θ_p is the rotation capacity of the plastic hinge formed at the RC wall base and ω_θ is a reduction factor included for the possible storey drift amplification due to higher modes of vibration. In the case of RC frames and braced frames, it is

assumed for simplicity here that these displaced shape expressions are representative at all damage states. Therefore, for a given value of θ_{max}, the corresponding Δ_i can be found and subsequently the Δ_d for each structural system. At the SLS where no ductile behaviour is anticipated, the values of $\Delta_{d,SLS}$ are computed.

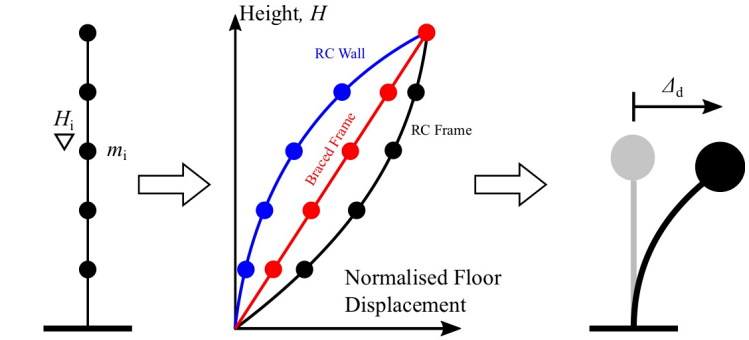

Figure 12. Identification of Δ_d for different structural systems.

Relating PFA to spectral acceleration, *Sa*, is a little trickier due to the nature of the problem where unlike θ_{max}, a_{max} cannot be assumed to be first mode dominated. Since the process of identifying a *Sa* for various building solutions assumes that the structure remains in the elastic range of response, some simplifications can be made. Consider that the j^{th} mode contribution to the PFA at the i^{th} floor for an elastically responding structure to be:

$$a_{i,j} = \phi_{i,j}\Gamma_j Sa(T_j) \tag{9}$$

where $Sa(T_j)$ is the spectral acceleration at the j^{th} mode period of vibration, $\phi_{i,j}$ is the j^{th} mode shape value at floor i and Γ_j is the j^{th} mode's participation factor, given by:

$$\Gamma_j = \frac{\sum_i m_i \phi_{i,j}}{\sum_i m_i \phi_{i,j}^2} \tag{10}$$

Combining the first few modes using a square-root-sum-of-the-squares (SRSS) combination gives the PFA profile along the height, a_i, with a maximum value of a_{max}. Knowing the structural typology as any one of those illustrated in Figure 12, it will tend to have relatively standardised mode shapes, meaning that the individual Γ values will remain somewhat constant since they depend on storey stiffness and floor mass distribution. Knowing the number of storeys and the structural typology, Equation (10) can be approximated by a single coefficient γ defined as:

$$\alpha_{SLS} \approx \gamma a_{max} \tag{11}$$

Initial parametric studies on the elastic modal properties of structures suggest that values of γ for low rise structures to be of the order of 0.70-0.80, 0.75-0.90 and 0.65-0.80 for RC frames, RC walls and braced frames, respectively. Future work should look to refine these coefficients for different typologies of differing number of storeys but for the purposes of conceptual design discussed here, they are deemed reasonable.

Using the values of $\Delta_{d,SLS}$ and α_{SLS}, these can be marked on the design SLS spectrum as in Figure 13, which results in a range bound by the two lines from the origin. Recalling that the slope of a line through the origin is directly related to the period of vibration, T, it becomes clear that in order to respect the SLS requirements, the eventual design solution must possess a first-mode period, T_1, within the zone highlighted in grey and bound by points 1 and 2 in Figure 13. This essentially implies that the structure must be stiff enough to not exhibit excessive deformation but be flexible enough so as not to generate excessive floor accelerations at the SLS.

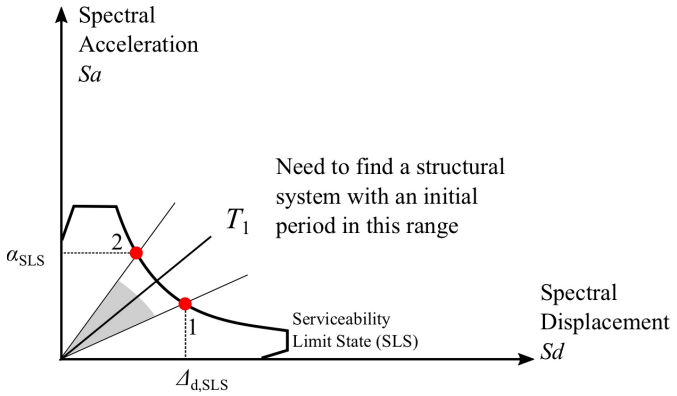

Figure 13. Identification of permissible initial secant to yield period range based on PFA and PSD limits for the SLS.

With the permissible period range known from Figure 13, two further pieces of information are required: the design displacement and the lateral strength. The lateral strength can be directly related to *Sa* by assuming first-mode dominated response, shown in Figure 14 as α_{ULS}, and is set as a trial value by the designer. Examining the latter aspect of design displacement, where the value of θ_{max} identified for the ULS can be converted to a design displacement, $\Delta_{d,ULS}$. This value of $\Delta_{d,ULS}$ is illustrated via point 3 and the area bound by points 1, 2 and 3 in Figure 14 represents the design solution space within which the final backbone behaviour must fall.

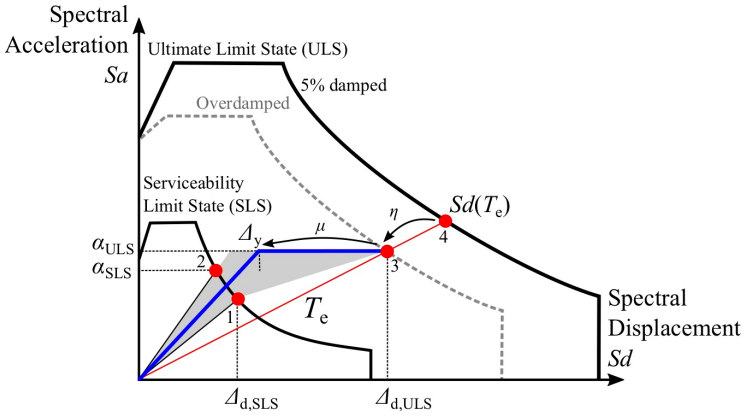

Figure 14. Identification of design solution space shaded in grey considering the permissible period range and the trialled value of lateral strength capacity.

At the ULS, the effects of system non-linearity need to be accounted for. Considering the effective period, T_e, passing from the origin through point 3 and comparing this expected capacity with the elastic spectral demand marked at point 4 in Figure 14, $Sd(T_e)$. The non-linear behaviour of the structure will be expected to account for this amplification in the structure's spectral capacity. The relationship between linear and non-linear behaviour in seismic design may be found via a modification to the elastic design spectrum by reducing or overdamping as a function of ductility, as shown in Figure 14. Since the design displacement, $\Delta_{d,ULS}$, and the elastic response spectrum are known, this required amplification of the structure's spectral capacity with respect to the elastic demand due to the non-linear behaviour is simply determined as:

$$\eta = \frac{\Delta_{d,ULS}}{Sd(T_e)} \tag{12}$$

Priestley *et al.* [19] outline a number of expressions for various structural systems characterised by different hysteretic models representative of different structural systems. Such relationships are plotted in Figure 15 using expressions proposed by Priestley *et al.* [19] and O'Reilly and Sullivan [31], for example. Using these kinds of plots, the required ductility, μ, can be identified by entering from the vertical axis with the required spectral modification factor, η, and reading off the corresponding value. For cases where the required η does not intersect the curve (e.g. η=0.50), this essentially implies that the structural system being examined is simply not capable of providing sufficient spectral reduction to sustain such a demand and the trial lateral strength needs to be modified.

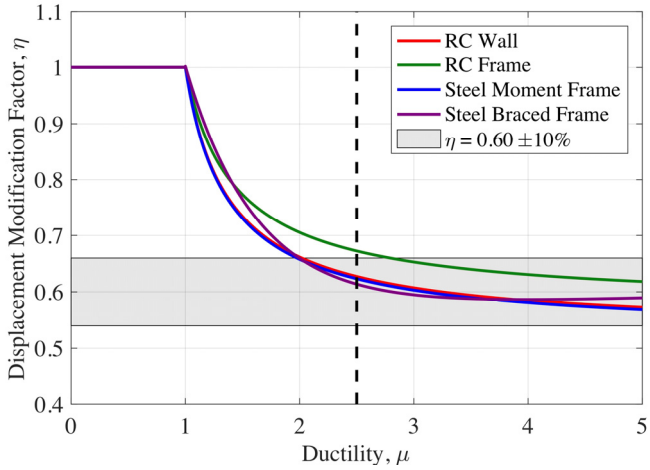

Figure 15. Displacement modification factors for some typical structural systems.

Knowing the value of η and its associated μ, the yield spectral displacement, Δ_y, of the structural system is computed as follows:

$$\Delta_y = \frac{\Delta_{d,ULS}}{\mu} \tag{13}$$

meaning that the final bilinear backbone of the structural system has been identified and is illustrated via the blue line in Figure 14. It is noted that the value of μ used in Equation (13) may also be determined from Figure 15 but can be taken as ≈ 2.5 initially.

As outlined in Figure 14, the design outputs from the proposed approach are α_{ULS}, μ and maximum Δ_y required to maintain compatibility with the identified performance objectives. α_{ULS} and μ are simply related to the provided strength of the dissipative zones in the eventual structural design, whereas Δ_y is related to the chosen structural system. Knowing Δ_y, the final dimensions and material properties of the structural system can be identified since it is well-known to be independent of the lateral strength [21]. Take an RC frame with a ductile beam-sway mechanism, for example, the yield drift, θ_y, has been shown by Priestley *et al.* [19] to be given by:

$$\theta_y = \frac{0.5\epsilon_y B}{h_b} \tag{14}$$

where B is the bay width of the frame and h_b is the beam depth. In the case of steel moment frames, Priestley *et al.* [19] noted that the coefficient in Equation (14) could simply be changed to 0.65. This can be then related to the Δ_y of the equivalent SDOF through the following relationship:

$$\Delta_y = \theta_y \frac{\sum_{i=1}^{n} m_i \Delta_i H_i}{\sum_{i=1}^{n} m_i \Delta_i} \tag{15}$$

where the expression describing the displaced shape was outlined in Equation (6) above. Similarly in the case of an RC wall, this can be computed in a similar fashion by modifying the expression in Equation (7) to give:

$$\Delta_y = \frac{\sum_{i=1}^{n} m_i \Delta_{y,i}^2}{\sum_{i=1}^{n} m_i \Delta_i} \tag{16}$$

where the yield displacement profile, $\Delta_{y,i}$, is given by:

$$\Delta_{y,i} = \frac{\epsilon_y H_i^2}{l_w}\left(1 - \frac{H_i}{3H_n}\right) \tag{17}$$

This results in the same situation where for an RC wall system to have a certain equivalent SDOF yield displacement Δ_y, the required length of wall and material properties can be established. Lastly in the case of braced frames, this may be computed as per Equation (15) above, where only a value of yield drift is needed. In the case of concentrically braced steel frames, this

may be computed following Wijesundara *et al.* [32] or O'Reilly and Sullivan [31] for the case of eccentrically braced steel frames.

This last step is relatively straightforward, whereby α_{ULS} is converted to a design base shear, V_{b}, and distributed along the structure height to result in design member forces as follows:

$$V_b = \alpha_{ULS} m_e = \alpha_{ULS} \frac{\Sigma_{i=1}^{n} m_i \Delta_i}{\Delta_{d,ULS}} \tag{18}$$

The term α_{ULS} can simply be thought of as being approximately equal to the design base shear coefficient since the V_{b} is found by the product of the effective mass, as shown in Equation (18).

DISCUSSION

Definition of design spectra

Regarding the definition of design spectra considering local soil effects as per Calvi and Andreotti [3], the main empirical references are the peak spectral accelerations (i.e. low periods), the peak spectral displacement (i.e. high periods) and the peak ordinates controlled by spectral velocity (i.e. mid periods). With this approach, it is possible to handle both spectral accelerations and spectral displacements within a single set of equations belonging to the same empirical model, with the following advantages: (*i*) the assumption of constant velocity used by traditional design spectra has been removed [1]; (*ii*) the conversion of spectral displacements from spectral accelerations is not needed; and (*iii*) it is possible to directly account for non-linear soil amplification effects.

This last aspect characterises the proposed model because, aiming to derive statistically more robust empirical equations (e.g. GMPEs), site-amplification models are often used to enable ground motions records from all site conditions, including non-rock stations. However, the majority of the recording stations are located on soil. This is the reason why semi-empirical amplification models are often used in the calibration of GMPEs for outcropping rock, in order to adjust the ordinates measured on soil. Directly accounting for non-linear soil amplification is still relatively uncommon for classical GMPEs because the empirical evidence of this phenomenon is considered rare [e.g. 33,34]. The empirical data presented in our study shows evidence of non-linear soil amplification effects that are directly included in the proposed predictive model. The possible causes of this difference have been identified in: (*i*) a different method of processing the empirical data (i.e. different method to combine the two horizontal components of the ground motions and the use of peak spectral ordinates instead of median values) and (*ii*) the use of a more updated version of ground motions database. According to other studies [35,36], the empirical data of our study also suggest that the simplified approaches for the definition of the seismic demand of Eurocode 8 [6,37] and the Italian Building Code [38] have the tendency to underestimate spectral accelerations and displacements.

Comparison of conceptual design framework with existing design codes

Examining the proposed framework, a number of improvements can be noted with respect to the limitations of current code prescriptions discussed previously. Current codes give relatively little explicit consideration to limit states other than the life safety requirement. Some checks may be present for non-structural elements at lower return periods but are widely known to be insufficient. Furthermore, the mitigation of excessive floor accelerations to protect non-structural elements and building contents is generally not given direct consideration. With respect to these limitations, the proposed design framework is a clear progression. It considers both drift and acceleration-sensitive elements at the SLS by identifying a suitable initial secant to yield period range.

Consider another aspect where a building's structural system is first identified and subsequently sized, the proposed framework is a significant improvement in this regard. The desired backbone performance is identified and the required structural geometry subsequently established. This is because the yield displacement of a system can be related back to structural dimensions and is relatively independent of the lateral strength. This follows the thinking that assuming constant lateral stiffness for variations of the same typology in FBD was illogical and, in fact, the yield displacement tends to remain constant.

Base isolation and supplemental damping: when to utilise them?

One area the proposed framework can be of great benefit to practitioners is in relation to the decision of when to use base isolation or supplemental damping. This is something very often decided by the engineer based on experience or as result of difficulty in finding a feasible solution. In the proposed framework, this would be more direct and obvious to designers because of the way performance objectives are set out. Consider those utilised previously for the SLS marked in Figure 16. If the case arose where the SLS demand were too large and a suitable period range could not be identified via an intersection with the design spectrum, this would indicate that additional measures are required. This is because it isn't possible for traditional systems to mitigate the displacements and accelerations at the SLS, whereas base isolation or supplemental damping would

reduce this design demand and permit more feasible solutions to be found. These aspects are to be developed further in future studies.

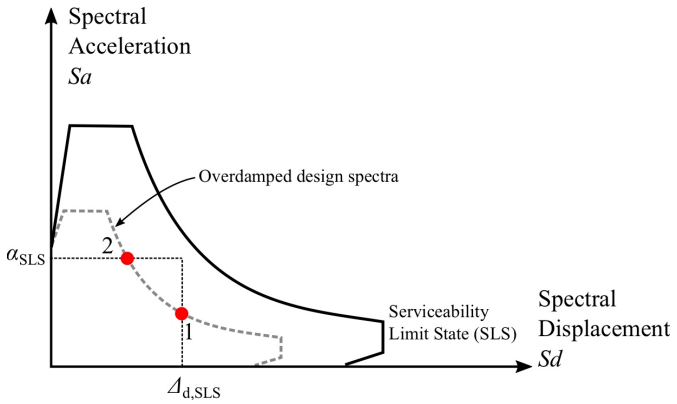

Figure 16. Example of when SLS performance objectives cannot be met and some solution in the form of base isolation or supplemental damping is required.

Consideration of indirect losses and downtime

Another potential development would be to consider indirect losses and downtime in the proposed design framework. The ELR values discussed previously referred exclusively to direct loss since y_{ULS} was set at 100% of the building replacement cost. Indirect losses may be incorporated through a more advanced ELR definition depending on the building occupancy type and its strategic role in society. For example, consider the total losses observed in a hypothetical building like a hospital in Figure 17. At the OLS, no indirect losses are anticipated and the total loss consists solely of the direct loss. With increasing damage to the building, the indirect losses begin to accumulate because of issues like having to set up temporary shelters or move patients to another facility at the SLS and ULS. Beyond the ULS, the direct losses will saturate, but the indirect losses may markedly increase due to the complete structural collapse and loss of life, for example. Considering these aspects, the losses associated with each limit state in Figure 9 and the target EAL may be adjusted to consider indirect losses at the design stage. In current design codes, importance factors are typically used meaning that the seismic input is amplified by a fixed coefficient to provide increased lateral resistance. It is argued that considering the importance of a building using total losses may be a more comprehensive and somewhat integrated approach.

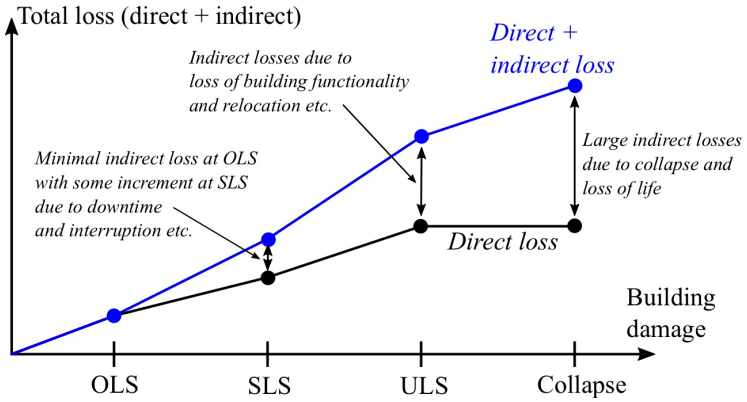

Figure 17. Evolution of total losses with increasing building damage, where potential sources of indirect losses are indicated with respect to the building damage. (Note: Vertical axis not to scale).

SUMMARY

A novel design framework utilising expected annual loss (EAL) to identify feasible structural solutions that align with the conceptual goals of performance-based design has been outlined. It is intended to form the first phase in the design process where the building is conceptually designed before being later detailed and verified with more detailed analysis. As with any

simplified method, a number of assumptions were needed. The first of these was the use of storey loss functions to convert expected loss ratios to design peak storey drift, θ_{max}, and peak floor acceleration, a_{max}. Two limit state intensities, serviceability (SLS) and ultimate limit states (ULS), were considered to characterise the structure's initial elastic and ductile non-linear behaviour. For the SLS, it was shown how θ_{max} and a_{max} can be used to characterise a permissible initial secant to yield period range. By trialling a lateral resistance and knowing the required system ductility for the ULS, the yield displacement of the system can be computed. Considering this with the acceptable period range, the design solution space can be identified and a potential bilinear backbone identified. Knowing that a structure's yield displacement depends primarily on material properties and geometry, the required dimensions of the structure can be identified as part of the first phase of design where the structural system and its layout are conceived.

The entire procedure is based on a more physical-based definition of input ground motions, which results in the definition of different forms of design spectra, immediately applicable, and a more rational definition of the effects of local soil on spectral shapes and values. Appropriate ways of accounting energy dissipation also resulted in a different proposed correction of elastic spectra.

ACKNOWLEDGEMENTS

The work presented in this paper has been developed within the framework of the project "Dipartimenti di Eccellenza", funded by the Italian Ministry of Education, University and Research at IUSS Pavia.

REFERENCES

1. Calvi GM. Revisiting design earthquake spectra. *Earthquake Engineering & Structural Dynamics* 2018; **47**(13): 2627–2643. DOI: 10.1002/eqe.3101.
2. Calvi GM, Rodrigues D, Silva V. Introducing new design spectra derived from Italian recorded ground motions 1972 to 2017. *Earthquake Engineering & Structural Dynamics* 2018; **47**(13): 2644–2660. DOI: 10.1002/eqe.3102.
3. Calvi GM, Andreotti G. Effects of local soil, magnitude and distance on response and design spectra. *Under Review* 2019.
4. Calvi GM. On the correction of spectra by a displacement reduction factor in direct displacement-based seismic design and assessment. *Earthquake Engineering & Structural Dynamics* 2019(January): 1–8. DOI: 10.1002/eqe.3159.
5. SEAOC. *Vision 2000: Performance-based seismic engineering of buildings*. Sacramento, California: 1995.
6. EN 1998-1:2004. *Eurocode 8: Design of Structures for Earthquake Resistance - Part 1: General Rules, Seismic Actions and Rules for Buildings*. Brussels, Belgium: 2004.
7. ASCE 7-16. *Minimum Design Loads for Buildings and Other Structures*. Reston, VA, USA: 2016.
8. NZS 1170.5:2004. *Structural Design Actions Part 5: Earthquake Actions - New Zealand*. Wellington, New Zealand: 2004.
9. Cornell CA, Krawinkler H. Progress and Challenges in Seismic Performance Assessment. *PEER Center News* 2000; **3**(2): 1–2.
10. FEMA P58-1. *Seismic Performance Assessment of Buildings: Volume 1 - Methodology (P-58-1)*. vol. 1. Washington, DC: 2012.
11. O'Reilly GJ, Perrone D, Fox M, Monteiro R, Filiatrault A. Seismic assessment and loss estimation of existing school buildings in Italy. *Engineering Structures* 2018; **168**: 142–162. DOI: 10.1016/j.engstruct.2018.04.056.
12. O'Reilly GJ, Calvi GM. Conceptual seismic design in performance-based earthquake engineering. *Earthquake Engineering & Structural Dynamics* 2019; **48**(4): 389–411. DOI: 10.1002/eqe.3141.
13. Andreotti, G., A. Famà and C.G. Lai (2018). Hazard-dependent soil factors for site-specific elastic acceleration response spectra of Italian and European seismic building codes. Bulletin of Earthquake Engineering, DOI: 10.1007/s10518-018-0422-9.
14. Seed HB, Ugas C, Lysmer J. Site-dependent spectra for earthquake-resistant design. *Bulletin of the Seismological Society of America* 1976; **66**(1): 221–243.
15. Seed HB, Idriss IM. Ground Motions and Soil Liquefaction during Earthquakes. *Earthquake Engineering Research Institute* 1982.
16. Akkar S, Sandıkkaya MA, Bommer JJ. Empirical ground-motion models for point- and extended-source crustal earthquake scenarios in Europe and the Middle East. *Bulletin of Earthquake Engineering* 2014; **12**(1): 359–387. DOI: 10.1007/s10518-013-9461-4.
17. Riddell R. Inelastic response spectrum: Early history. *Earthquake Engineering & Structural Dynamics* 2008; **37**(8): 1175–1183. DOI: 10.1002/eqe.810.
18. Newmark NM, Hall JF. *Earthquake specta design*. Berkeley, California: 1982.
19. Priestley MJN, Calvi GM, Kowalsky MJ. *Displacement Based Seismic Design of Structures*. Pavia, Italy: IUSS Press; 2007.

20. Freeman SA. Prediction of Response of Concrete Buildings to Severe Earthquake Motion. *Douglas McHenry International Symposium on Concrete and Concrete Structures*, Detroit, Michigan: 1978.
21. Priestley MJN. Myths and Fallacies in Earthquake Engineering, Revisited. *The 9th Mallet Milne Lecture*, Pavia, Italy: IUSS Press; 2003.
22. Taghavi S, Miranda E. Response Assessment of Nonstructural Building Elements. *PEER Report 2003/05* 2003.
23. Welch DP, Sullivan TJ. Nonstructural Considerations for Seismic Serviceability Performance in European Steel Moment Frames. *Giornate Italiane della Costruzione in Acciaio*, Torino, Italia: 2013.
24. Decreto Ministeriale. *Linee Guida per la Classificazione del Rischio Sismico delle Costruzioni - 58/2017*. Rome, Italy: 2017.
25. Calvi GM, Sullivan TJ, Welch DP. A seismic performance classification framework to provide increased seismic resilience. *2nd European Conference on Earthquake Engineering and Seismology*, Istanbul, Turkey: 2014.
26. Dolce M, Manfredi G. *Libro bianco sulla ricostruzione privata fuori dai centri storici nei comuni colpiti dal sisma dell'Abruzzo del 6 aprile 2009*. Doppiavoce, Napoli, Italy: 2015.
27. Shahnazaryan D, O'Reilly GJ, Monteiro R. Using direct economic losses and collapse risk for seismic design of RC buildings. *COMPDYN 2019 - 7th International Conference on Computational Methods in Structural Dynamics and Earthquake Engineering*, Crete Island, Greece: 2019.
28. Cornell CA, Jalayer F, Hamburger RO, Foutch DA. Probabilistic Basis for 2000 SAC Federal Emergency Management Agency Steel Moment Frame Guidelines. *Journal of Structural Engineering* 2002; **128**(4): 526–533. DOI: 10.1061/(ASCE)0733-9445(2002)128:4(526).
29. Pinto PE, Franchin P. Existing Buildings: The New Italian Provisions for Probabilistic Seismic Assessment. In: Ansal A, editor. *Perspectives on European Earthquake Engineering and Seismology*, Springer; 2014. DOI: 10.1007/978-3-319-07118-3_3.
30. Ramirez CM, Miranda E. Building Specific Loss Estimation Methods & Tools for Simplified Performance Based Earthquake Engineering. *Blume Report No 171* 2009.
31. O'Reilly GJ, Sullivan TJ. Direct Displacement-Based Seismic Design of Eccentrically Braced Steel Frames. *Journal of Earthquake Engineering* 2016; **20**(2): 243–278. DOI: 10.1080/13632469.2015.1061465.
32. Wijesundara KK, Bolognini D, Nascimbene R, Calvi GM. Review of Design Parameters of Concentrically Braced Frames with RHS Shape Braces. *Journal of Earthquake Engineering* 2009; **13**(sup1): 109–131.
33. Bindi D, Massa M, Luzi L, Ameri G, Pacor F, Puglia R, *et al.* Pan-European ground-motion prediction equations for the average horizontal component of PGA, PGV, and 5 %-damped PSA at spectral periods up to 3.0 s using the RESORCE dataset. *Bulletin of Earthquake Engineering* 2014; **12**(1): 391–430. DOI: 10.1007/s10518-013-9525-5.
34. Douglas J, Edwards B. Recent and future developments in earthquake ground motion estimation. *Earth-Science Reviews* 2016; **160**: 203–219. DOI: 10.1016/j.earscirev.2016.07.005.
35. Pitilakis K, Riga E, Anastasiadis A. New code site classification, amplification factors and normalized response spectra based on a worldwide ground-motion database. *Bulletin of Earthquake Engineering* 2013; **11**(4): 925–966. DOI: 10.1007/s10518-013-9429-4.
36. Andreotti G, Famà A, Lai CG. Hazard-dependent soil factors for site-specific elastic acceleration response spectra of Italian and European seismic building codes. *Bulletin of Earthquake Engineering* 2018; **16**(12): 5769–5800. DOI: 10.1007/s10518-018-0422-9.
37. EN 1998-1:2018. *Eurocode 8: Design of Structures for Earthquake Resistance (Draft) - Part 1: General Rules, Seismic Actions and Rules for Buildings*. Brussels: 2018.
38. NTC. *Norme Tecniche Per Le Costruzioni*. Rome, Italy: 2018.